Environmental Science & Technology

pubs.acs.org/est

Article

Traceable Calibration of Atmospheric Oxidized Mercury Measurements

Tyler R. Elgiar, Seth N. Lyman,* Teodor D. Andron, Lynne Gratz, A. Gannet Hallar, Milena Horvat, Sreekanth Vijayakumaran Nair, Trevor O'Neil, Rainer Volkamer, and Igor Živković

Cite This: https://doi.org/10.1021/acs.est.4c02209

Read Online

ACCESS | Metrics & More | Article Recommendations | Supporting Information

ABSTRACT: Most previous measurements of oxidized mercury were collected using a method now known to be biased low. In this study, a dual-channel system with an oxidized mercury detection limit of 6−12 pg m^{-3} was deployed alongside a permeation tube-based automated calibrator at a mountain top site in Steamboat Springs Colorado, USA, in 2021 and 2022. Permeation tubes containing elemental mercury and mercury halides were characterized via an International System of Units (SI)-traceable gravimetric method and gas chromatography/mass spectrometry before deployment in the calibrator. The dual-channel system recovered 97 ± 4 and 100 ± 8% (±standard deviation) of injected elemental mercury and $HgBr_2$, respectively. Total Hg permeation rates and Hg speciation from the gravimetric method, the chromatography system, the dual-channel system, and an independent SI-traceable measurement method performed at the Jožef Stefan Institute laboratory were all comparable within the respective uncertainties of each method. These are the first measurements of oxidized mercury at low environmental concentrations that have been verified against an SI-traceable calibration system in field conditions while sampling ambient air, and they show that accurate, routinely calibrated oxidized mercury measurements are achievable.

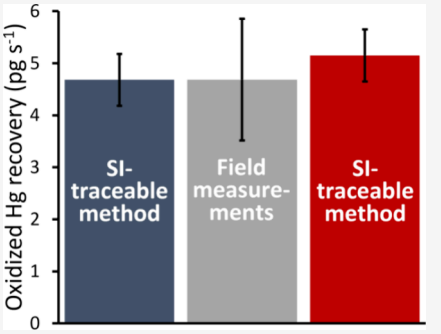

KEYWORDS: *atmosphere, mercury, elemental, oxidized, calibration*

1. INTRODUCTION

Mercury (Hg) is a globally distributed, neurotoxic, trace metal that can harm the ecosystem, wildlife, and human health.[1,2] Found ubiquitously throughout the environment, Hg occurs naturally and is present in three main forms, elemental Hg (Hg^0), inorganic Hg, and organic Hg[3]. The effects of Hg exposure vary significantly based on dosage, duration, individual susceptibility, and the form of Hg involved. These factors can impact neurological and cardiovascular systems, highlighting the complexity of the health effects of Hg.[2,4] Prenatal exposure to Hg has been linked to neurological disorders such as autism and may hinder fetal development.[5−7] Human exposure to Hg primarily occurs through the consumption of contaminated food, especially fish and rice.[8,9]

Most Hg pollution is emitted to the atmosphere via natural (e.g., biomass burning and volcanic eruptions) and anthropogenic (e.g., coal burning power plants and artisanal gold mining) sources.[10−12] Mercury is present in the atmosphere as either gaseous elemental Hg (Hg^0), gaseous oxidized Hg, or particle-bound oxidized Hg. In this work, the sum of gaseous oxidized Hg and particle-bound oxidized Hg will be referred to as Hg^{II} because the measurements discussed do not differentiate between the two (and quantitative differentiation may be impossible with currently available instrumentation; Lyman et al.[13]). Once in the atmosphere, Hg undergoes complex oxidation and reduction chemistry, dynamically converting between Hg^0 and Hg^{II}.[14,15] Elemental Hg has an atmospheric lifetime of up to one year and is subject to global transport and deposition.[16−18] Oxidized Hg is soluble,[19] more reactive, and is thus easily deposited to earth's surface.[13] Once deposited, Hg can be converted to toxic organic Hg species and become subject to bioaccumulation and biomagnification.[20,21]

Hg^{II} is present at ultratrace levels in the atmosphere (low pg m^{-3}), making it difficult to measure accurately and precisely. Measurements of atmospheric Hg^{II} were previously made with commercial systems that utilized a KCl-coated denuder, which is now known to be biased low.[22−26] Cation exchange membrane-based systems appear to avoid the low bias created by the KCl denuder and have been deployed at many locations around the globe.[27−29] Most measurements of Hg^{II} have been uncalibrated, however, including those made with cation exchange membranes, making it difficult to assess their validity. A few groups have investigated methods to quantitatively calibrate measurements of Hg^{II}, but further standardization studies are needed.[30−34] A recent review assessed that

Received: March 1, 2024
Revised: May 31, 2024
Accepted: June 3, 2024

permeation tube-based systems are the best candidate currently available to calibrate ambient Hg^{II} measurements,[33] and permeation tube-based calibrators have previously been utilized in field settings.[27,35−37]

In this study, we aimed to evaluate the stability and traceability of a permeation tube-based calibrator for Hg measurements under ambient field conditions. Specifically, a cation exchange membrane-based dual-channel Hg^0 and Hg^{II} measurement system was deployed alongside an automated permeation tube-based calibrator at Storm Peak Laboratory in the Rocky Mountains of Colorado, USA. The permeation rates of the permeation tubes were characterized in two separate laboratories by International System of Units (SI)-traceable gravimetric analysis, GC/MS, and SI-traceable cold vapor atomic fluorescence analysis. Our objective was to determine whether these permeation tube-based systems can provide stable, traceable calibration for ambient Hg measurements. Detailed analyses of the measurement data are reported separately.[38,39] We hypothesized that the permeation tube-based calibrator would demonstrate consistent and reliable performance, providing SI-traceable calibration for both Hg^0 and Hg^{II} measurements. Notably, we are unaware of any other Hg^{II} measurements that have been verified during ambient air sampling in field conditions with SI-traceable calibration, making this study potentially groundbreaking in the field of mercury atmospheric chemistry.

2. METHODS

2.1. Sampling Location. Measurements were collected during two separate periods (12 March to 10 October 2021 and 3 March to 22 September 2022) at Storm Peak Laboratory (SPL) in Steamboat Springs Colorado, USA[40,41] (Figure S9). SPL is a permanent atmospheric monitoring station situated on top of the Steamboat Ski Resort (3220 m above sea level; 40.455, −106.744).

2.2. Dual-Channel System. Ambient Hg^0 and Hg^{II} were measured at 10 min time resolution using a dual-channel Hg measurement system developed at Utah State University (Figure S1) and based on systems used in several previous studies.[27,35,42] The dual-channel system pulled air through a heated inlet (110 °C) at a total flow of 9 L min^{-1}. The inlet contained an elutriator and quartz particle impactor with a 50% cut point at 2.5 μm aerodynamic diameter. After the elutriator and impactor, the instrument pulled sample air at 1 L min^{-1} into two separate channels. One channel contained a thermal converter heated to 650 °C that converted all Hg in the sample air into Hg^0, giving a measurement of total Hg. The thermal converter used in this study was identical to the one tested by Lyman and Jaffe,[43] except the converter tube was packed with quartz chips instead of quartz wool. The other channel contained a series of two 47 mm diameter cation exchange membranes (Pall Corporation, Mustang S; 0.8 μm pore size) in a PFA Teflon filter holder. The cation exchange membranes collected Hg^{II} and allowed Hg^0 to pass through,[44] producing a measurement of only Hg^0. Flow from one channel at a time was routed into a Tekran 2537X Hg^0 analyzer, while the flow from the other channel was routed through a mass flow controller, a pump, and then vented. The Tekran analyzer collected measurements on each of its gold traps at 2.5 min intervals and switched between the two channels at 5 min intervals. Hg^{II} was calculated as the difference between the two channels (total Hg − Hg^0 = Hg^{II}). A separate PTFE valve was used to occasionally route air coming from the thermal converter upstream of the cation exchange membranes to determine whether bias existed between the two channels and to calculate a detection limit for Hg^{II}.

A similar dual-channel system has been used in previous studies.[27,35,42] The dual-channel system used in this study differed in a few significant ways. First, the inlet line of the dual-channel system was shortened to less than 1 m to minimize loss of Hg^{II}. This required housing the membranes and thermal converter inside a weatherproof box on top of the sampling shelter, rather than indoors. The inlet line was constructed of PFA tubing (6.4 mm OD) and was heated to 110 °C upstream of the thermal converter and CEMs. Another difference is that the Tekran 2537X used in the current system was selected by the manufacturer for high sensitivity to improve the detection limit and was modified by the manufacturer to decrease dead volume. A new, custom-designed inlet was also used to allow for a robust connection to the calibrator.

Additional information about the dual-channel system is available in the Supporting Information.

2.3. Permeation Tubes. Hg measurements were calibrated using a permeation tube-based calibrator. The permeation tubes[27,37] (Figure S3) were constructed from PTFE Teflon tubing of approximately 3 mm outer diameter and 2 cm length, with a wall thickness of 0.8 mm. Small amounts of liquid Hg^0 (Sigma-Aldrich, purity >99.9%) or crystalline $HgBr_2$ or $HgCl_2$ (American Elements, purity >99.9%) were placed between two PTFE plugs at both ends of the tubing and pushed together to create a permeable length of about 1 mm (this length varied slightly among permeation tubes). Some Hg^0 permeation tubes were constructed using a solid PTFE cylinder of approximately the same dimensions with a small hole (∼1.5 mm in diameter) drilled in it where a small amount of liquid Hg^0 was placed. This cylinder was placed inside a piece of PTFE tubing with a wall thickness of 0.2 mm. This created a smaller permeable area, decreasing the permeation rate. A permeation tube that held no Hg was constructed and used as a blank. All permeation tubes in this study were kept at 70.0 ± 0.1 °C.

Previous work has shown that $HgBr_2$ and $HgCl_2$ behave similar to each other in analytical and calibration systems.[27,37,45] The chemical speciation of atmospheric Hg^{II} is not known with certainty,[13] and Hg halide compounds were used in this work because they are commercially available and can reasonably be expected to comprise a significant portion of ambient atmospheric Hg.[46] However, most of the work presented here involves $HgBr_2$ (rather than $HgCl_2$) permeation tubes because $HgBr_2$ was found to pass more efficiently through the GC/MS system (Figure S11), simplifying its characterization. Future work will focus on $HgCl_2$ and nonhalide Hg compounds.

2.4. Characterization of Permeated Hg Speciation. A gas chromatograph/mass spectrometer (GC/MS; Shimadzu QP2010 Ultra) and sample processing system were used to determine the speciation of Hg permeated from the permeation tubes (Figure S4). This was the same GC/MS system used by Jones et al.[45] and allowed for selection among multiple permeation tubes and cryogenic concentration of Hg followed by thermal release of Hg into the GC/MS. Outputs from the permeation tubes could be routed through a thermal converter to convert Hg^{II} compounds into Hg^0 prior to cryogenic concentrations and analysis. Hg^{II} compounds were efficiently trapped at 0 °C, while Hg^0 was trapped at −100 °C.

https://doi.org/10.1021/acs.est.4c02209
Environ. Sci. Technol. XXXX, XXX, XXX−XXX

Permeation tubes to be analyzed were placed in a permeation oven kept at 70.0 ± 0.1 °C, which connected to the GC/MS system. He was usually used as the carrier gas, and flow orifices to control He flow were placed upstream of permeation tubes.

Hg^{II} compounds were trapped and analyzed to qualitatively assess their identity from their mass spectra. Since no independent Hg^{II} standard exists, however, quantitative determination of the speciation of permeated Hg was done using Hg^0. This was accomplished by trapping the output from Hg^{II} permeation tubes at −100 °C with and without thermal conversion to Hg^0. The Hg^0 mass (determined from the peak area) when the output was not thermally converted was assumed to represent the percent of total permeated Hg that was Hg^0; the Hg^0 mass when the output was thermally converted was assumed to represent total permeated Hg, and the percent of total Hg that was Hg^{II} was determined by the difference between these two values. The system was calibrated by injecting Hg^0 vapor through a syringe.

Additional information about the GC/MS system is available in the Supporting Information.

2.5. Gravimetric Characterization of Permeation Rates. Permeation tubes were removed from the permeation oven at weekly or semiweekly intervals and weighed with a Mettler Toledo microbalance (Model XS3DU; 1 μg readability).[27] SI-traceable mass standards (200 and 500 mg) were used to verify the accuracy of the microbalance before each weighing of permeation tubes. Microbalance results were only considered valid if measurements of the standards were within 3 μg of the nominal mass. To mitigate static interference, the permeation tubes were passed through a static dissipater (Mettler Toledo 63052302 Haug Deionizer) several times before being weighed. Even after passing through the static dissipater, the tubes often retained some static charge, as evidenced by significant changes across successive weighings. If successive weighings were inconsistent, tubes were passed through the static dissipater again and then weighed successively again. This process continued until at least two consecutive measurements were within 2 μg of each other. While outside of the permeation oven, the permeation tubes were transported in glass vials and handled only with either Teflon-wrapped stainless steel or Teflon-coated tweezers.

Permeation rates were determined from a linear regression of mass loss versus elapsed time, and all mass loss from the tubes was assumed to be due to loss of Hg^0 or Hg^{II} compounds. Mass loss rates for Hg compounds were converted to Hg^0 loss rates before comparison with other Hg measurements.

2.6. Calibrator. An automated calibrator (Figure S8) was used to calibrate Hg^{II} and Hg^0 measurements made by the dual-channel system. This was the same calibrator used by Dunham-Cheatham et al.[35] After characterization in the laboratory via GC/MS and gravimetric analysis, the permeation tubes were placed inside the calibrator. The calibrator housed permeation tubes in a permeation oven heated to 70.0 ± 0.1 °C that was similar to the one described for the GC/MS, except that UHP N_2 was used as a carrier gas and a Sulfinert-coated stainless steel flow orifice (Lenox Laser; PN SS-1/4−17) was used downstream of the permeation tubes to control flow, rather than upstream, to maintain a constant pressure for the permeation tubes. The permeation oven connected to valves that selected among permeation tubes and between two different heated outlet lines and all materials were Sulfinert-coated stainless steel except the valve rotors, which were constructed of Valcon E.

Continuous flow of Hg^{II} compounds from the permeation tubes would result in Hg concentrations well above ambient levels in the dual-channel system, leading to contamination. The calibrator was used in two different modes to overcome this problem. In the first mode (automated), Hg flowed for a preprogrammed number of seconds into the inlet of the dual-channel system during each 2.5 min gold-trap cycle of the Tekran 2537X. After the preprogrammed Hg injection, the multiport valve switched to flush the outlet line with only UHP N_2 for the remainder of the gold-trap cycle. The calibrator continued to inject for the same number of seconds for each gold-trap cycle for a preprogrammed period (usually 2 or 3 h).

In the alternative, manual mode, one of the calibrator's output lines was disconnected from the dual-channel inlet and continuously release permeated Hg into ambient air away from the dual-channel inlet for at least 2 h. This allowed for complete equilibration of the permeated Hg with the calibrator's valves and tubing. After 2 h, the still-flowing calibrator outlet line was manually inserted into the tip of the dual-channel system's inlet for 10 s during each gold-trap cycle of the Tekran 2537X, while the dual-channel sampled ambient air (results were corrected for Hg in ambient air). This accomplished the same purpose as the automated mode but allowed equilibration of the calibrator lines before injection. Some Hg^{II} remained in the dual-channel inlet after each manual mode injection and flushed out over a period of 15−20 min. Thus, the dual channel was allowed to pull ambient air after each set of injections for at least 30 min, and Hg concentrations above background (determined as the average of values prior to injection) during this period were added to the amount of Hg recovered.

2.7. Atomic Fluorescence Measurements at Jožef Stefan Institute. The calibrator was installed in a laboratory at the Jožef Stefan Institute for an added, independent comparison. It was used in manual mode, with the output flowing continuously for at least several hours prior to sampling. When not used for sampling, the outlet tip of the calibrator was inserted loosely into a 6 mm-diameter PTFE tube that was connected to a vacuum pump with a flow of about 1 L min^{-1} to vent the calibrator output outdoors.

Analysis was performed using cold vapor atomic fluorescence spectrometry (CV-AFS). The fluorescence detector was calibrated using the NIST 3133 standard reference material (Hg^{2+} in an acidified aqueous solution). Appropriate masses of diluted NIST 3133 were pipetted into an impinger (pipettes were directly calibrated with diluted NIST 3133 solution by pipetting 10 consecutive aliquots and weighing the corresponding masses). A solution of 10% $SnCl_2$ (w/v) in 10% HCl (v/v) was used to reduce the Hg^{2+} in the reference material to Hg^0. After the $SnCl_2$ solution was added, the impinger was immediately capped and purged with UHP N_2 gas for 4 min at 50 mL min^{-1} to quantitatively purge out the Hg^0, which was then collected on a gold-coated silica trap. A soda lime trap was placed before the gold trap to dry Hg vapors. After purging, the gold trap was placed in a double amalgamation system, which thermally desorbed the Hg^0 from the gold trap, and a stream of Ar carried the analyte to the AFS detector.

The same gold trap used for calibration was also used for sampling the Hg^0 and Hg^{II} outputs from the calibrator. The calibrator's output line was loosely inserted for either 30, 60, or 90 s into the gold-coated silica trap approximately 2 cm

https://doi.org/10.1021/acs.est.4c02209
Environ. Sci. Technol. XXXX, XXX, XXX−XXX

upstream from the quartz wool that held the gold-coated silica in place. A suction pump, connected to the other side of the gold-coated silica trap, was used to pull the output from the calibrator through the trap. By using a suction pump and loosely inserted calibrator's output line, we ensured that vacuum was not directly pulling Hg from the calibrator. Different suction flows were tested (7−50 mL min^{-1}), but no differences were observed at any flow.

When sampling $HgBr_2$, an Al_2O_3 sand trap was placed upstream of the gold trap to collect Hg^{II}. Hg collected on the Al_2O_3 trap was considered to be Hg^{II}, while Hg collected on the gold trap was considered to be Hg^0, as Hg^0 does not attach to inert surfaces such as Al_2O_3. The Al_2O_3 trap method was chosen because it was shown to be successful in previous work as a collection medium for laboratory-generated Hg^{II}, and Hg^{II} compounds have been shown to be efficiently thermally desorbed from the material.[30] After the gold trap was analyzed for the Hg^0 breakthrough, Hg^{II} on the Al_2O_3 trap was thermally reduced at 600 °C under an Ar stream, volatilized, and collected on the same gold trap that was analyzed previously. Hg^{II} was then quantified in the same manner as Hg^0 using AFS. Collection of Hg^{II} by the Al_2O_3 trap was tested by converting a NIST-traceable quantity of Hg^0 to Hg^{II} using the cold plasma method described by Gačnik et al.[30]

All measurements were corrected for the corresponding procedural blanks. Output from the calibrator's blank permeation tube was <0.01% of output from the Hg-containing permeation tubes.

2.8. Measurement Uncertainty. Detection limits for the dual-channel system were calculated as three times the standard deviation of Hg^{II} measurements during times that air from the thermal converter was routed to the membrane channel, so both channels sampled the same Hg^{II}-free air. This was done for 3 h during each week of measurements.

Standard and expanded uncertainties were calculated for the dual-channel instrument and the other measurement methods utilized in this study, following methods in the NIST Engineering Statistics Handbook[47] and the method of Brown et al.[48] Details of the methods used are available in the Supporting Information.

2.9. Units and Statistical Presentations. A value of 0.05 was used for α when determining statistical significance. Data are presented as averages ±95% confidence intervals where appropriate. Exceptions are indicated in the text.

This text refers to the Hg permeation rate, the rate of Hg mass loss from permeation tubes, in units of pg s^{-1}. The gravimetric permeation rate was determined from the change in permeation tube mass over time. The permeation rate recovered by Hg measurement instrumentation is also referred to and was determined as the mass of Hg measured by the instrument per second of Hg injection by the calibrator, regardless of the Hg species. For injections into ambient air (including all the reported data for the dual-channel system), ambient Hg^0 and Hg^{II} concentrations from the 20 min period prior to injection were subtracted from the injection period prior to calculating the recovered permeation rate.

3. RESULTS AND DISCUSSION

3.1. Measurement Uncertainty. 1-h average ambient air detection limits of Hg^{II} measurements averaged 12 ± 7 pg m^{-3} and 6 ± 2 pg m^{-3} during the first and second measurement periods, respectively. Since Hg^{II} measurements relied on total Hg and Hg^0 measurements, the Hg^{II} detection limits are assumed to be an upper bound for the detection limits of total Hg and Hg^0. Recovery of Hg^0 by the Tekran 2537X when Hg^0 was manually injected from a saturated vapor source was 101 ± 6%.

Expanded uncertainties (k = 2, equivalent to approximately 95% confidence) calculated for the methods used in this work are shown in Table 1.

Table 1. Expanded Uncertainties for the Measurement Methods Used in This Study[a]

	reference measured value	expanded uncertainty	percent expanded uncertainty
gravimetric perm. rate Hg^0	11.5 pg s^{-1}	0.8 pg s^{-1}	7%
gravimetric perm. rate $HgBr_2$	4.7 pg s^{-1}	0.5 pg s^{-1}	10%
GC-MS Hg^0	356 pg	90 pg	25%
GC-MS Hg^{II}	4685 pg	946 pg	20%
GC-MS Hg^{II}/total Hg	0.93	0.18	19%
JSI CV-AFS Hg^0	78 pg	11 pg	14%
JSI CV-AFS Hg^{II}	386 pg	38 pg	10%
JSI total Hg perm. rate	5.2 pg s^{-1}	0.5 pg s^{-1}	10%
JSI Hg^{II}/total Hg	0.80	0.08	10%
dual-channel Hg^0	1200 pg m^{-3}	196 pg m^{-3}	16%
dual-channel Hg^{II}	100 pg m^{-3}	16 pg m^{-3}	16%
dual-channel total Hg perm. rate	4.7 pg s^{-1}	1.1 pg s^{-1}	25%
dual-channel Hg^{II}/ total Hg amb.	0.08	0.01	12%

[a]Reference measured values used in uncertainty calculations are indicated. JSI is Jožef Stefan Institute. Permeation rates are shown for $HgBr_2$ permeation tube #1027 and Hg^0 permeation tube #1033 (Table S1).

The uncertainty of the gravimetric permeation rate depended on the number of successive weighings and the time period over which successive weighings occurred. For the results shown in Table 1, seven weighings occurred at two-week intervals.

Uncertainties do not include possible loss or transformation of Hg^0 and Hg compounds during transmission through calibration and measurement instrumentation. Dual-channel uncertainties incorporate uncertainty due to calibration via manual Hg vapor injections, rather than calibration via the permeation tube-based calibrator, so the calibrator uncertainty can be shown separately. Also, the uncertainty of dual-channel Hg measurements depended on Hg concentrations. Table 1 shows uncertainty at 100 pg m^{-3} Hg^{II}. At 20 pg m^{-3} Hg^{II}, expanded uncertainty rises to 44%.

3.2. Ambient Hg Measurements. Figure 1 shows that values for Hg^{II} were occasionally negative. This may have occurred due to (1) rapid changes in ambient Hg^0 since total Hg and Hg^0 were not measured simultaneously or (2) contamination in the Hg^0 channel. When operating earlier versions of the dual-channel system,[27,35,42] persistent negative Hg^{II} measurements occasionally occurred and were rectified by changing the cation exchange membranes or cleaning the channel. These negative Hg^{II} values were thus presumed to be caused by contamination of the cation exchange membrane channel. In the current study, however, negative Hg^{II} was never persistent, indicating either (1) contamination did not occur

https://doi.org/10.1021/acs.est.4c02209
Environ. Sci. Technol. XXXX, XXX, XXX−XXX

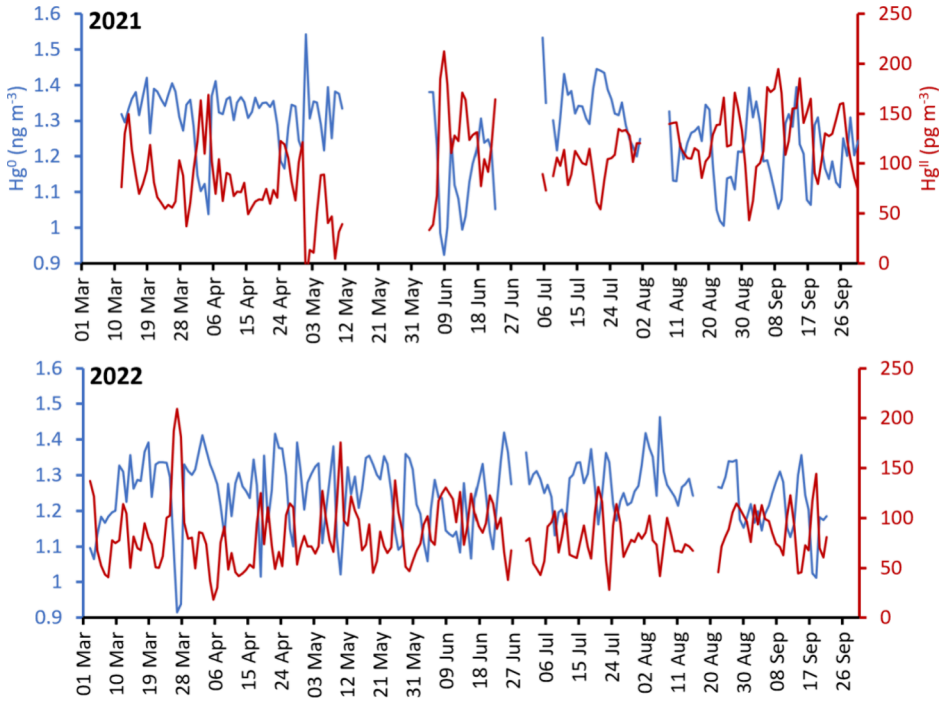

Figure 1. Daily average Hg^0 and Hg^{II} measurements during the 2021 (top) and 2022 (bottom) measurement periods.

and negative values were due to rapid changes in ambient Hg^0 or (2) contamination did occur but was intermittent.

Previous Hg measurements at SPL by Fain et al.[40] showed an average Hg^{II} concentration of 20 pg m^{-3} and multiple events with high Hg^{II}, including an Hg^{II} maximum of 137 pg m^{-3}. The Hg^{II} measurements in the Fain et al. study were made with a KCl-coated denuder-based system, which is known to be biased low. Hourly averaged Hg^{II} concentrations measured by the dual-channel system in the current study were up to five times higher than previous measurements at SPL. The maximum 1-h average Hg^{II} concentration during this study was 520 pg m^{-3}. A brief data summary for both measurement periods compared to Fain et al.[40] is presented in Table 2.

Table 2. Average and Maximum Concentrations for Hg^0 and Hg^{II} from Fain et al.[40] and during Both Dual-Channel System Measurement Periods from This Study[a]

	Mar 12−Oct 10 2021	Mar 03−Sep 22 2022	Fain et al.
average Hg^0 (ng m^{-3})	1.26 ± 0.13	1.25 ± 0.11	1.6 ± 0.3
average Hg^{II} (pg m^{-3})	103 ± 50	84 ± 34	20 ± 21
max Hg^0 (ng m^{-3})	2.38	1.67	5.0
max Hg^{II} (pg m^{-3})	520	239	137

[a]All values are shown as average ±1 standard deviation.

Further analyses of the measurements collected with the dual-channel system, including comparisons with other measurements collected at SPL, analyses of air mass origins and characteristics, and comparisons with photochemical models, are available separately.[38,39] The main focus of this paper is the development of methods for SI-traceable verification of the Hg measurements, and subsequent sections focus on this topic.

3.3. Results for Different Calibrator Configurations.

Information about each permeation tube used in this work, and additional information about calibrator and permeation tube performance, are available in Table S1 and associated discussion in the Supporting Information. Total Hg recovered by the dual-channel system from permeation tubes used during the 2021 deployment period (see Table S1 for a description of all permeation tubes used and their deployment periods) was less than 5% of the amount expected based on the gravimetrically determined permeation rate. The tubes were characterized gravimetrically while in the GC/MS system. As noted in the Methods, the GC/MS system used He as a carrier gas and had flow orifices placed upstream of the permeation tubes, while the calibrator used N_2 with downstream orifices. The calibrator was returned to the laboratory and connected to the GC/MS system to investigate this discrepancy. The calibrator was tested using He and N_2 carrier gases and by moving the flow orifices between the upstream and downstream positions. The permeation tubes were allowed to equilibrate for at least 24 h after any change to the system was made, and the calibrator output flowed continuously through the GC/MS system before, during, and after sampling by the GC/MS system.

Figure 2 shows that GC/MS-determined permeation rates for $HgBr_2$ and Hg^0 permeation tubes decreased when N_2 was used as the carrier gas and when the flow orifice was downstream of the tubes. For the $HgBr_2$ tube, the percentage of total Hg emitted from the tube that was recovered by the GC/MS as $HgBr_2$ decreased from 99 to 93% when the flow orifice position was changed from upstream to downstream of the permeation tube (Figure S14).

Other studies have shown that in a steady state, the permeation rate from a given permeation tube is dependent only on temperature.[49−54] If this is true, a change in the carrier

https://doi.org/10.1021/acs.est.4c02209
Environ. Sci. Technol. XXXX, XXX, XXX−XXX

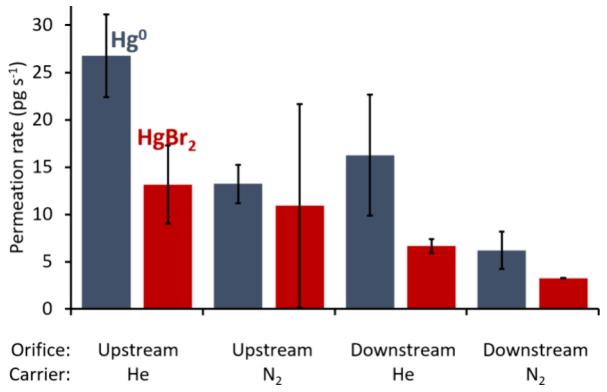

Figure 2. Permeation rate of $HgBr_2$ and Hg^0 permeation tubes determined via GC/MS with different carrier gases and flow orifice positions. Whiskers show 95% confidence intervals.

gas flow rate, as could be expected when switching the carrier gas but keeping the flow orifice the same, is not expected to change the permeation rate after equilibration is achieved. Some studies have shown an increase in permeation rate with increased flow rate for non-Hg permeation tubes,[55,56] however. In this study, different carrier gas flow rates (15.1−41.7 mL min^{-1}) for an $HgBr_2$ permeation tube in the GC/MS system showed no significant change in observed permeation rate (Figure S15), except at the highest flow rates tested. We hypothesize that the lower observed permeation rate at the highest flow was due to reduced $HgBr_2$ collection efficiency during cryogenic concentration.

Changing the position of the flow orifice from upstream to downstream of the permeation tube increased the pressure experienced by the permeation tube. However, Jost[53] showed that, after adequate equilibration time, the permeation rate is not affected by pressure. Only permeation devices containing compounds subject to decomposition in a pressure-dependent equilibrium are likely to be affected by pressure.[53] To our knowledge, there have been no studies to determine if Hg^{II} compounds decompose in a pressure-dependent matter. Even if this is true for the $HgBr_2$ permeation tube, it does not explain why the emission rate of the Hg^0 tube changed when the flow orifice position changed since it cannot undergo molecular decomposition.

The causes of the observed impact of changes to the orifice position and carrier gas on permeation rate thus remain unclear. Nevertheless, these findings (1) elucidate part of the reason for the discrepancy between gravimetrically determined and dual-channel recovered permeation rates during the 2021 deployment period and (2) underscore the importance of holding all conditions constant when comparing laboratory and field results for Hg-containing permeation tubes. Lyman et al.[27] found good agreement between field and laboratory tests with a permeation tube-based calibrator, but they used the same calibrator, with the same configuration and conditions, in all tests, and they only compared the relative difference between lab and field recovery of Hg, rather than comparing against GC/MS-based and gravimetric characterizations. After the 2021 deployment period in the current study, carrier gases and orifice positions were kept the same for the calibrator and the GC/MS system (i.e., N_2, downstream) when comparing results for the two systems.

3.4. Long Equilibration Times Needed. When the calibrator was in automated mode (i.e., discontinuous injections interspersed with N_2 flushing) in the dual-channel system at Storm Peak Laboratory, shorter injection times led to lower recovered permeation rates and a lower percentage of total Hg recovered as Hg^{II} (Figure S16). Even for a 41 s injection time, total recovered Hg was much less than expected from gravimetric and GC/MS results. This was true even when injections were repeated for each gold-trap cycle of the Tekran 2537X over periods of several hours, and it was true for both $HgBr_2$ and Hg^0. Thus, it appears that long equilibration times with continuous flow from the calibrator are needed and that the calibrator's automated mode was ineffective. Figure S11 shows that many repeat injections of $HgCl_2$ were needed to flush $HgBr_2$ from the GC/MS system and for $HgCl_2$ peaks to stabilize, providing more evidence for the need for system equilibration prior to injecting Hg^{II} compounds.

3.5. Hg Recovery by the Dual-Channel System. Because automated mode did not allow for equilibration under continuous flow conditions, the calibrator was used in manual mode during the 2022 field season, with at least 2 h of equilibration prior to use. When the calibrator was used in this way, the dual-channel system recovered 100 ± 25 and 97 ± 22% of the gravimetrically determined $HgBr_2$ and Hg^0 permeation rates, respectively (Figure 3; ± expanded

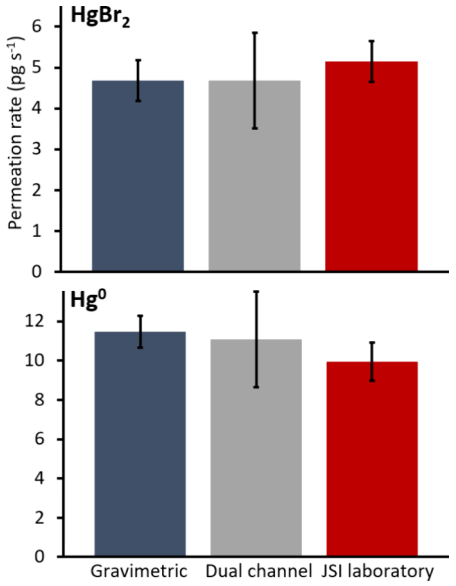

Figure 3. Total Hg permeation rate of $HgBr_2$ and Hg^0 permeation tubes determined gravimetrically, from recovery of Hg added from the calibrator (manual mode) while the dual-channel system sampled ambient air at Storm Peak Laboratory, and via SI-traceable atomic fluorescence detection at the Jožef Stefan Institute laboratory. Whiskers show expanded uncertainties.

uncertainty; confidence intervals were 4% for both permeation tubes). Permeation rates determined by atomic fluorescence at the Jožef Stefan Institute laboratory were not significantly different from those determined by the dual-channel system and the gravimetric method (Figure 3). Dual-channel measurements included a correction for a suspected bias in the Dumarey equation used for calculating saturated Hg vapor concentrations, while measurements at the Jožef Stefan Institute laboratory did not. A discussion of the implications of this difference is available in the Supporting Information.

The percent of Hg detected by the dual-channel system as Hg^{II} during $HgBr_2$ calibrations in manual mode was 96 ± 3%

https://doi.org/10.1021/acs.est.4c02209
Environ. Sci. Technol. XXXX, XXX, XXX−XXX

(±95% confidence interval), compared to 93 ± 1% for injections from the calibrator into the GC/MS (Figure 4). The

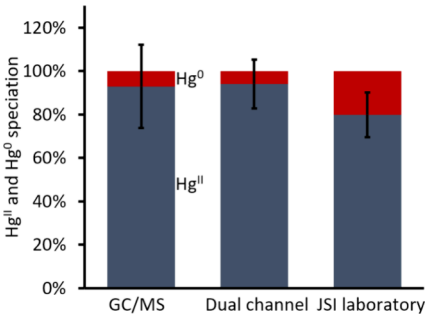

Figure 4. Percent Hg^{II} and Hg^0 recovered from the same $HgBr_2$ permeation tube when injected by the calibrator (manual mode) into the GC/MS, the dual-channel system while it sampled ambient air at Storm Peak Laboratory, and the atomic fluorescence system at the Jožef Stefan Institute laboratory. Whiskers show expanded uncertainties for percent Hg^{II}.

GC/MS and dual-channel systems recovered about 15% more of the Hg injected by the calibrator from an $HgBr_2$ permeation tube as Hg^{II} than the system used at the JoŽef Stefan Institute, but the differences were not significant. All three systems use different methods to differentiate between Hg^{II} and Hg^0. While the gravimetric method and the Hg detection method used at the Institute are SI-traceable with respect to total Hg, none of the methods of differentiation between Hg^{II} and Hg^0 can be considered to be SI-traceable. The Hg^{II} collection efficiency of the Al_2O_3 traps used at the Jožef Stefan Institute was tested against the SI-traceable cold plasma Hg^{II} generation method, but the method does not involve ambient air collection of Hg^{II}, so the collection efficiency of the Al_2O_3 traps in ambient air, as they were used when collecting $HgBr_2$ from the calibrator, is unknown.

The portion of total Hg that is Hg^{II}, as well as any possible transformations of Hg^{II} compounds in a measurement or calibration system, is difficult to verify independently since no independent, gas-phase standards exist that emit either pure Hg^{II} or known concentrations of both Hg^{II} and Hg^0 in the ambient concentration range. Preliminary work with the GC/MS system has shown that some thin-wall (0.2 mm wall thickness) $HgBr_2$ permeation tubes in the GC/MS system (with He as the carrier gas and flow orifices upstream of tubes) emit less than 1% of total Hg as Hg^0. SI-traceable verification of a high-purity Hg^{II} source could be accomplished relatively simply by (1) showing the absence of a significant Hg^0 signal and (2) determining the Hg^{II} permeation rate gravimetrically or by thermally converting Hg^{II} to Hg^0 and then analyzing by SI-traceable methods for Hg^0. For such an Hg^{II} source to be useful, however, conversion of permeated Hg^{II} to Hg^0 within the calibration system that delivers permeated Hg^{II} to an analyzer would need to be insignificant, and this is not currently possible.

3.6. Implications. As determined by the detection limit, the dual-channel-based measurements presented here are the most precise continuous Hg^{II} measurements that have been published. KCl denuder-based measurements have lower detection limits,[57] but they are biased low,[23−26,58] and the extent of the bias changes with ambient conditions,[13,37] so measurements collected with KCl denuders cannot be considered quantitative. The dual-channel system performed reliably in harsh field conditions and quantitatively recovered Hg^0 and Hg^{II} delivered by a SI-traceable calibration system in ambient air. This shows that cation exchange-based, dual-channel systems are a viable replacement for automated KCl denuder-based systems. However, more work is needed to ensure that cation exchange-based dual-channel systems perform quantitatively in a variety of field conditions. SI-traceable calibrations of such systems in humid and urban environments are especially needed since these environments are very different from the high-elevation, low-humidity, mostly rural environments where dual-channel systems have been calibrated thus far (Lyman et al.[27] and Dunham-Cheatham et al.[35]). Calibration with nonhalide Hg compounds is also needed.

The first evidence that KCl denuder-based methods are biased low for Hg^{II}[25] did not surface until about a decade after the methods were in widespread use because of no established field calibration method for Hg^{II}. SI-traceable, field-deployable, routine calibrations of Hg^{II} in ambient air have been called for in the literature since 2014[58] but have not been carried out successfully until this study. As a variety of new methods for ambient air Hg^{II} are developed and deployed, routine calibrations like these will be essential. Vijayakumaran Nair et al.[34] presented an SI-traceable calibration method that involves loading KCl denuders with nonthermal, plasma-generated Hg^{II} in the lab and desorbing them in the field. Their calibration method could be adapted to other measurement methods that trap and then analyze Hg^{II}, such as the RMAS system,[29] and it could incorporate ambient air sampling of the loaded denuders or other collection surfaces to increase robustness. It will not work for indirect, continuous methods like the dual-channel system presented here.

Routine field calibrations of Hg^0 are needed that are independent, SI-traceable, and occur in ambient air at the inlet tip. Manual syringe injections are sometimes carried out at the inlet tip, but these are based on saturated Hg vapor equations that have discrepancies and are not SI-traceable.[34,59−61] The methods presented here can be used for routine Hg^0 calibrations in addition to Hg^{II}.

While this study represents a significant step forward for ambient Hg measurements and calibrations, challenges remain. Key remaining measurement challenges include the following:

1. The dual-channel system does not differentiate between gas- and particle-phase Hg^{II}. A different inlet design is needed to ensure a clear size cut for particle-phase Hg^{II},[13] and an added channel or some other method would be needed to measure particle-phase Hg^{II} separate from gaseous Hg^{II}.
2. The dual-channel system makes no attempt to determine the chemical composition of Hg^{II} compounds. While cation exchange membranes have been tested for many Hg^{II} compounds,[22,24,62] it is possible that some ambient Hg^{II} compounds are not quantitatively analyzed by the system.
3. Because the dual-channel system measures total Hg and Hg^0 asynchronously, it may calculate spuriously high or low Hg^{II} if total Hg or Hg^0 is changing rapidly. This means that the detection limit is highly dependent on variability in ambient Hg. A system that either switches between channels rapidly or samples both channels synchronously and then analyzes each one asynchronously is needed. A two-detector system has been used

https://doi.org/10.1021/acs.est.4c02209
Environ. Sci. Technol. XXXX, XXX, XXX−XXX

to solve this problem,[43,63−65] but this increases the expense and complexity of measurements, and may also lead to poorer detection limits.

Key remaining calibration challenges include the following:

1. The gravimetric verification method requires Hg permeation rates that are too high for continuous injection into an analyzer, and the automated short-duration method attempted in this study was unsuccessful. Dynamic dilution methods are under development, which could overcome this obstacle and allow for automated injections at concentrations relevant to ambient air.
2. Since the speciation of ambient Hg^{II} compounds is not known with certainty, it is not known whether Hg halide compounds are adequate surrogates for Hg compounds that exist in ambient air. Gravimetrically verified nonhalide Hg permeation tubes are under development, and these would allow for calibration with Hg compounds that have a wider range of chemical and physical properties.
3. The total Hg permeation rate of the permeation tubes considered in this work can be considered SI-traceable, but the percent of permeated Hg that is Hg^{II} cannot. An Hg^{II} permeation tube field calibrator system that emits an insignificant amount of Hg^0 would alleviate this problem and may be possible.

While more work is needed, this study shows that it is possible to collect accurate, SI-traceable measurements of ambient Hg^0 and Hg^{II}. Such measurements are critically needed to accurately assess the sources, chemistry, and environmental impacts of Hg pollution. Article 22 of the Minamata Convention on Mercury calls for provision of "comparable monitoring data on the presence and movement of mercury and mercury compounds in the environment'.[66] This study provides the first set of methods by which ambient measurements of atmospheric Hg and Hg^{II} compounds in particular are routinely calibrated in real field conditions and can be considered "comparable" to SI standards, allowing for a quantitative understanding of atmospheric Hg cycling.

■ ASSOCIATED CONTENT

Supporting Information

The Supporting Information is available free of charge at https://pubs.acs.org/doi/10.1021/acs.est.4c02209.

Additional experimental and methodological details, as well as ancillary information and results, including diagrams of USU's dual channel system and the PTFE Teflon-coated aluminum inlet for the dual channel system, example photographs of $HgBr_2$ and Hg^0 permeation tubes, diagram of the GC/MS system, chromatogram and mass spectrum of output from an $HgBr_2$ permeation tube, peak area response to manual injections, diagram of the automated calibrator, location of Storm Peak Laboratory and the location of the dual channel system and automated calibrator on top of the laboratory's roof, uncertainty calculations, list of permeation tubes used in this study, gravimetrically determined total mass loss of the permeation tubes used in the 2021 and 2022 deployments, consecutive analyses ("runs") of an $HgCl_2$ permeation tube via the GC/MS system, permeation rate (determined with the GC/MS system) versus permeation oven temperature, Hg^0 and Hg^{II} recovery by the GC/MS, Hg^0 peak area detected by the MS at different flow rates of He, permeation rate recovered by the GC/MS versus recovery by the dual channel from short duration automated injections, permeation rate and percent of total Hg recovered as Hg^{II}, impact of adjustments for the Dumarey equation (PDF)

■ AUTHOR INFORMATION

Corresponding Author

Seth N. Lyman − *Bingham Research Center, Utah State University, Vernal, Utah 84078, United States; Department of Chemistry and Biochemistry, Utah State University, Logan, Utah 84322, United States;* orcid.org/0000-0001-8493-9522; Email: seth.lyman@usu.edu

Authors

Tyler R. Elgiar − *Bingham Research Center, Utah State University, Vernal, Utah 84078, United States*

Teodor D. Andron − *Jožef Stefan Institute, Ljubljana 1000, Slovenia; Jožef Stefan International Postgraduate School, Ljubljana 1000, Slovenia*

Lynne Gratz − *Reed College, Portland, Oregon 97202, United States*

A. Gannet Hallar − *Department of Atmospheric Sciences, University of Utah, Salt Lake City, Utah 84112, United States*

Milena Horvat − *Jožef Stefan Institute, Ljubljana 1000, Slovenia; Jožef Stefan International Postgraduate School, Ljubljana 1000, Slovenia*

Sreekanth Vijayakumaran Nair − *Jožef Stefan Institute, Ljubljana 1000, Slovenia; Jožef Stefan International Postgraduate School, Ljubljana 1000, Slovenia*

Trevor O'Neil − *Bingham Research Center, Utah State University, Vernal, Utah 84078, United States*

Rainer Volkamer − *Department of Chemistry & CIRES, University of Colorado Boulder, Boulder, Colorado 80309, United States;* orcid.org/0000-0002-0899-1369

Igor Živković − *Jožef Stefan Institute, Ljubljana 1000, Slovenia; Jožef Stefan International Postgraduate School, Ljubljana 1000, Slovenia;* orcid.org/0000-0003-1774-1203

Complete contact information is available at: https://pubs.acs.org/10.1021/acs.est.4c02209

Notes

The authors declare no competing financial interest.

Ambient air data collected during this project is publicly available (Gratz et al.[67]).

After the first and corresponding authors, all other authors are credited in alphabetical order. T.E.: instrument development, data collection, analysis, writing, edits. S.L.: project conceptualization, instrument conceptualization and development, data collection, analysis, uncertainty analysis, writing, edits. T.A.: analyses at Jožef Stefan Institute, edits. L.G.: project conceptualization, data collection, analysis, edits. A.H.: project conceptualization, data collection, edits. M.H.: analyses at Jožef Stefan Institute, edits. S.N.: analyses at Jožef Stefan Institute, writing, edits. T.O.: instrument development, data collection. R.V.: project conceptualization, edits. I.Z.: analyses at Jožef Stefan Institute, writing, edits.

https://doi.org/10.1021/acs.est.4c02209
Environ. Sci. Technol. XXXX, XXX, XXX−XXX

■ ACKNOWLEDGMENTS

This work was supported by NSF Grants # AGS 1951632, AGS-1951513, and AGS-1951515. The authors appreciate the assistance of Ian McCubbin and Dan Gilchrist, staff at Storm Peak Laboratory, for technical assistance with the installation and operation of the dual-channel Hg instrument and permeation tube-based automated calibrator. The Steamboat Ski Resort provided logistical support and in-kind donations. The University of Utah is a permittee of the Medicine-Bow Routt National Forests and is an equal opportunity service provider and employer. Davis Smuin and Jackson Leisik, undergraduate student researchers at Utah State University's Bingham Research Center, took part in laboratory measurements and testing. Pamela Gardner at the Bingham Research Center provided textual edits. Work at the Jožef Stefan Institute received financial support from the European Commission (GMOS-Train, #860497), the Marie Skłodowska-Curie Initial Training Network, and the Slovenian Research and Innovation Agency (ARIS, #P1-0143). The authors thank the Metrology Institute of the Republic of Slovenia (MIRS) under contract no. C3212-10-000071 (6401-5/2009/27) for activities and obligations performed as a Designate Institute.

■ REFERENCES

(1) Mahbub, K. R.; Krishnan, K.; Naidu, R.; Andrews, S.; Megharaj, M. Mercury toxicity to terrestrial biota. *Ecological Indicators* **2017**, *74*, 451−462.

(2) Rice, K. M.; Walker, E. M., Jr; Wu, M.; Gillette, C.; Blough, E. R. Environmental mercury and its toxic effects. *Journal of preventive medicine and public health* **2014**, *47* (2), 74.

(3) Carocci, A.; Rovito, N.; Sinicropi, M. S.; Genchi, G. Mercury toxicity and neurodegenerative effects. *Reviews of environmental contamination and toxicology* **2014**, *229*, 1−18.

(4) Hu, X. F.; Lowe, M.; Chan, H. M. Mercury exposure, cardiovascular disease, and mortality: A systematic review and dose-response meta-analysis. *Environmental research* **2021**, *193*, No. 110538.

(5) Zahir, F.; Rizwi, S. J.; Haq, S. K.; Khan, R. H. Low dose mercury toxicity and human health. *Environmental toxicology and pharmacology* **2005**, *20* (2), 351−360.

(6) Netto, B. B.; da Silva, E. P.; de Aguiar da Costa, M.; de Rezende, V. L.; Bolan, S. J.; Ceretta, L. B.; Aschner, M.; Dominguini, D.; Gonçalves, C. L. Critical period of exposure to mercury and the diagnostic of autism spectrum disorder: A systematic review. *Journal of Neurochemistry* **2024**, 1−13.

(7) Golding, J.; Rai, D.; Gregory, S.; Ellis, G.; Emond, A.; Iles-Caven, Y.; Hibbeln, J.; Taylor, C. Prenatal mercury exposure and features of autism: a prospective population study. *Mol. Autism* **2018**, *9* (1), 30.

(8) dos Santos Vianna, A.; de Matos, E. P.; de Jesus, I. M.; Asmus, C. I. R. F.; de Magalhães Câmara, V. Human exposure to mercury and its hematological effects: a systematic review. *Cad. Saude Publica* **2019**, *35*, No. e00091618.

(9) Zhang, H.; Feng, X.; Larssen, T.; Qiu, G.; Vogt, R. D. In inland China, rice, rather than fish, is the major pathway for methylmercury exposure. *Environ. Health Perspect.* **2010**, *118* (9), 1183−1188.

(10) Mason, R. P. Mercury emissions from natural processes and their importance in the global mercury cycle. In *Mercury Fate and Transport in the Global Atmosphere: Emissions, Measurements and Models*; Springer: Verlag New York 2009; pp 173−191.

(11) Pacyna, E. G.; Pacyna, J.; Sundseth, K.; Munthe, J.; Kindbom, K.; Wilson, S.; Steenhuisen, F.; Maxson, P. Global emission of mercury to the atmosphere from anthropogenic sources in 2005 and projections to 2020. *Atmos. Environ.* **2010**, *44* (20), 2487−2499.

(12) Munthe, J.; Kindbom, K.; Parsmo, R.; Yaramenka, K. *Technical Background Report to the Global Mercury Assessment 2018*. IVL Svenska Miljöinstitutet: 2019.

(13) Lyman, S. N.; Cheng, I.; Gratz, L. E.; Weiss-Penzias, P.; Zhang, L. An updated review of atmospheric mercury. *Sci. Total Environ.* **2020**, *707*, No. 135575.

(14) Lam, K. T.; Wilhelmsen, C. J.; Schwid, A. C.; Jiao, Y.; Dibble, T. S. Computational Study on the Photolysis of BrHgONO and the Reactions of BrHgO● with CH4, C2H6, NO, and NO2: Implications for Formation of Hg (II) Compounds in the Atmosphere. *J. Phys. Chem. A* **2019**, *123*, 1637−1647.

(15) Jiao, Y.; Dibble, T. S. First kinetic study of the atmospherically important reactions BrHg+ NO 2 and BrHg+ HOO. *Phys. Chem. Chem. Phys.* **2017**, *19* (3), 1826−1838.

(16) Lin, C.-J.; Pehkonen, S. O. The chemistry of atmospheric mercury: a review. *Atmos. Environ.* **1999**, *33* (13), 2067−2079. (acccessed 6/1).

(17) Ariya, P. A.; Amyot, M.; Dastoor, A.; Deeds, D.; Feinberg, A.; Kos, G.; Poulain, A.; Ryjkov, A.; Semeniuk, K.; Subir, M.; Toyota, K. Mercury physicochemical and biogeochemical transformation in the atmosphere and at atmospheric interfaces: A review and future directions. *Chem. Rev.* **2015**, *115* (10), 3760−3802.

(18) Si, L.; Ariya, P. A. Recent advances in atmospheric chemistry of mercury. *Atmos.* **2018**, *9* (2), Review. 76 Scopus.

(19) Sander, R. Compilation of Henry's law constants (version 5.0. 0) for water as solvent. *Atmos. Chem. Phys.* **2023**, *23* (19), 10901−12440.

(20) Morel, F. M. M.; Kraepiel, A. M. L.; Amyot, M. The chemical cycle and bioaccumulation of mercury. *Annual review of ecology and systematics* **1998**, *29*, 543.

(21) Lavoie, R. A.; Jardine, T. D.; Chumchal, M. M.; Kidd, K. A.; Campbell, L. M. Biomagnification of mercury in aquatic food webs: a worldwide meta-analysis. *Environ. Sci. Technol.* **2013**, *47* (23), 13385−13394.

(22) Huang, J.; Gustin, M. S. Uncertainties of Gaseous Oxidized Mercury Measurements Using KCl-Coated Denuders, Cation-Exchange Membranes, and Nylon Membranes: Humidity Influences. *Environ. Sci. Technol.* **2015**, *49* (10), 6102−6108.

(23) McClure, C. D.; Jaffe, D. A.; Edgerton, E. S. Evaluation of the KCl denuder method for gaseous oxidized mercury using HgBr2 at an in-service AMNet site. *Environ. Sci. Technol.* **2014**, *48* (19), 11437−11444.

(24) Huang, J.; Miller, M. B.; Weiss-Penzias, P.; Gustin, M. S. Comparison of gaseous oxidized Hg measured by KCl-coated denuders, and nylon and cation exchange membranes. *Environ. Sci. Technol.* **2013**, *47* (13), 7307−7316.

(25) Lyman, S. N.; Jaffe, D. A.; Gustin, M. S. Release of mercury halides from KCl denuders in the presence of ozone. *Atmos. Chem. Phys.* **2010**, *10* (17), 8197−8204.

(26) Bu, X.; Zhang, H.; Lv, G.; Lin, H.; Chen, L.; Yin, X.; Shen, G.; Yuan, W.; Zhang, W.; Wang, X.; Tong, Y. Comparison of Reactive Gaseous Mercury Collection by Different Sampling Methods in a Laboratory Test and Field Monitoring. *Environmental Science and Technology Letters* **2018**, *5* (10), 600−607. Article. Scopus.

(27) Lyman, S. N.; Gratz, L. E.; Dunham-Cheatham, S. M.; Gustin, M. S.; Luippold, A. Improvements to the accuracy of atmospheric oxidized mercury measurements. *Environ. Sci. Technol.* **2020**, *54* (21), 13379−13388.

(28) Tang, Y.; Wang, S.; Li, G.; Han, D.; Liu, K.; Li, Z.; Wu, Q. Elevated gaseous oxidized mercury revealed by a newly developed speciated atmospheric mercury monitoring system. *Environ. Sci. Technol.* **2022**, *56* (12), 7707−7715.

(29) Gustin, M. S.; Dunham-Cheatham, S. M.; Allen, N.; Choma, N.; Johnson, W.; Lopez, S.; Russell, A.; Mei, E.; Magand, O.; Dommergue, A.; Elgiar, T. Observations of the chemistry and concentrations of reactive Hg at locations with different ambient air chemistry. *Sci. Total Environ.* **2023**, *904*, No. 166184.

(30) Gačnik, J.; Živković, I.; Ribeiro Guevara, S.; Kotnik, J. e.; Berisha, S.; Vijayakumaran Nair, S.; Jurov, A.; Cvelbar, U.; Horvat, M.

https://doi.org/10.1021/acs.est.4c02209
Environ. Sci. Technol. XXXX, XXX, XXX−XXX

Calibration Approach for Gaseous Oxidized Mercury Based on Nonthermal Plasma Oxidation of Elemental Mercury. *Anal. Chem.* **2022**, *94* (23), 8234−8240.
(31) Sari, S.; Timo, R.; Jussi, H.; Panu, H. Dynamic calibration method for reactive gases. *Measurement Science and Technology* **2020**, *31* (3), No. 034001.
(32) Feng, X.; Lu, J. Y.; Hao, Y.; Banic, C.; Schroeder, W. H. Evaluation and applications of a gaseous mercuric chloride source. *Anal. Bioanal. Chem.* **2003**, *376* (7), 1137−1140.
(33) Davis, M.; Lu, J. Calibration Sources for Gaseous Oxidized Mercury: A Review of Source Design, Performance, and Operational Parameters. *Critical Reviews in Analytical Chemistry* **2022**, 1−10.
(34) Vijayakumaran Nair, S.; Gačnik, J.; Živković, I.; Andron, T. D.; Ali, S. W.; Kotnik, J.; Horvat, M. Application of traceable calibration for gaseous oxidized mercury in air. *Anal. Chim. Acta* **2024**, *1288*, No. 342168.
(35) Dunham-Cheatham, S. M.; Lyman, S.; Gustin, M. S. Comparison and calibration of methods for ambient reactive mercury quantification. *Sci. Total Environ.* **2023**, *856*, No. 159219.
(36) Finley, B. D.; Jaffe, D. A.; Call, K.; Lyman, S.; Gustin, M. S.; Peterson, C.; Miller, M.; Lyman, T. Development, testing, and deployment of an air sampling manifold for spiking elemental and oxidized mercury during the Reno Atmospheric Mercury Intercomparison Experiment (RAMIX). *Environ. Sci. Technol.* **2013**, *47* (13), 7277−7284.
(37) Lyman, S.; Jones, C.; O'Neil, T.; Allen, T.; Miller, M.; Gustin, M. S.; Pierce, A. M.; Luke, W.; Ren, X.; Kelley, P. Automated Calibration of Atmospheric Oxidized Mercury Measurements. *Environ. Sci. Technol.* **2016**, *50* (23), 12921−12927.
(38) Derry, E. J.; Elgiar, T.; Wilmot, T. Y.; Hoch, N. W.; Hirshorn, N. S.; Weiss-Penzias, P.; Lee, C. F.; Lin, J. C.; Hallar, A. G.; Volkamer, R.; Lyman, S. N.; Gratz, L. E. Elevated oxidized mercury in the free troposphere: Analytical advances and application at a remote continental mountaintop site. *EGUsphere* **2024**, *2024*, 1−42.
(39) Lee, C. F.; Eligar, T.; David, L. M.; Wilmot, T. Y.; Reza, M.; Hirshorn, N.; McCubbin, I. B.; Shah, V.; Lin, J. C.; Lyman, S. Elevated Tropospheric Iodine over the Central Continental United States: Is Iodine a Major Oxidant of Atmospheric Mercury? *ESS Open Archive* **2024**. DOI: 10.22541/essoar.171136849.98199430/v1.
(40) Fain, X.; Obrist, D.; Hallar, A. G.; McCubbin, I.; Rahn, T. High levels of reactive gaseous mercury observed at a high elevation research laboratory in the Rocky Mountains. *Atmos. Chem. Phys.* **2009**, *9* (20), 8049−8060.
(41) Hallar, A. G.; Petersen, R.; McCubbin, I. B.; Lowenthal, D.; Lee, S.; Andrews, E.; Yu, F. *Climatology of new particle formation and corresponding precursors at Storm Peak Laboratory*. 2016.
(42) Lyman, S. N.; Elgiar, T.; Gustin, M. S.; Dunham-Cheatham, S. M.; David, L. M.; Zhang, L. Evidence against Rapid Mercury Oxidation in Photochemical Smog. *Environ. Sci. Technol.* **2022**, *56* (16), 11225−11235.
(43) Lyman, S. N.; Jaffe, D. A. Elemental and oxidized mercury in the upper troposphere and lower stratosphere. *Nature Geoscience* **2012**, *5*, 114−117.
(44) Miller, M. B.; Dunham-Cheatham, S. M.; Gustin, M. S.; Edwards, G. C. Evaluation of cation exchange membrane performance under exposure to high Hg0 and HgBr2 concentrations. *Atmos. Meas. Technol.* **2019**, *12* (2), 1207−1217. Article. Scopus.
(45) Jones, C. P.; Lyman, S. N.; Jaffe, D. A.; Allen, T.; O'Neil, T. L. Detection and quantification of gas-phase oxidized mercury compounds by GC/MS. *Atmos. Meas. Technol.* **2016**, *9* (5), 2195−2205.
(46) Shah, V.; Jacob, D. J.; Thackray, C. P.; Wang, X.; Sunderland, E. M.; Dibble, T. S.; Saiz-Lopez, A.; Černušák, I.; Kellö, V.; Castro, P. J.; Wu, R.; Wang, C. Improved mechanistic model of the atmospheric redox chemistry of mercury. *Environ. Sci. Technol.* **2021**, *55* (21), 14445−14456.
(47) NIST. *NIST/SEMATCH e-Handbook of Statistical Methods*; 2012. DOI: 10.18434/M32189.
(48) Brown, R. J.; Brown, A. S.; Yardley, R. E.; Corns, W. T.; Stockwell, P. B. A practical uncertainty budget for ambient mercury vapour measurement. *Atmos. Environ.* **2008**, *42* (10), 2504−2517.
(49) Saltzman, B. E.; Burg, W. R.; Ramaswamy, G. Performance of permeation tubes as standard gas sources. *Environ. Sci. Technol.* **1971**, *5* (11), 1121−1128.
(50) Deighton, M.; Williams, S.; Lassey, K.; Hannah, M.; Boland, T.; Eckard, R.; Moate, P. Temperature, but not submersion or orientation, influences the rate of sulphur hexafluoride release from permeation tubes used for estimation of ruminant methane emissions. *Animal Feed Science and Technology* **2014**, *194*, 71−80.
(51) Mitchell, G. D. A review of permeation tubes and permeators. *Separation and Purification Methods* **2000**, *29* (1), 119−128.
(52) Lucero, D. P. Performance characteristics of permeation tubes. *Anal. Chem.* **1971**, *43* (13), 1744−1749.
(53) Jost, C. Calibration with permeation devices: is there a pressure dependence of the permeation rates? *Atmos. Environ.* **2004**, *38* (21), 3535−3538. (acccessed 7).
(54) Saltzman, B. E.; Burg, W. R.; Cuddeback, J. E. Continuous monitoring instrument for reactive hydrocarbons in ambient air. *Anal. Chem.* **1975**, *47* (13), 2234−2238. ; M3: doi: 10.1021/ac60363a045 (acccessed 11/01).
(55) Susaya, J.; Kim, K.-H.; Cho, J.; Parker, D. The controlling effect of temperature in the application of permeation tube devices in standard gas generation. *Journal of Chromatography A* **2012**, *1225*, 8−16.
(56) Susaya, J.; Kim, K.-H.; Cho, J. W.; Parker, D. The use of permeation tube device and the development of empirical formula for accurate permeation rate. *Journal of Chromatography A* **2011**, *1218* (52), 9328−9335.
(57) Poissant, L.; Pilote, M.; Beauvais, C.; Constant, P.; Zhang, H. H. A year of continuous measurements of three atmospheric mercury species (GEM, RGM and Hg p) in southern Quebec, Canada. *Atmos. Environ.* **2005**, *39* (7), 1275−1287.
(58) Jaffe, D. A.; Lyman, S.; Amos, H. M.; Gustin, M. S.; Huang, J.; Selin, N. E.; Levin, L.; Ter Schure, A.; Mason, R. P.; Talbot, R.; Rutter, A.; Finley, B.; Jaeglé, L.; Shah, V.; McClure, C. D.; Ambrose, J. L.; Gratz, L.; Lindberg, S.; Weiss-Penzias, P.; Sheu, G. R.; Feddersen, D.; Horvat, M.; Dastoor, A.; Hynes, A.; Mao, H.; Sonke, J. E.; Slemr, F.; Fisher, J. A.; Ebinghaus, R.; Zhang, Y.; Edwards, G. Progress on understanding atmospheric mercury hampered by uncertain measurements. *Environ. Sci. Technol.* **2014**, *48* (13), 7204−7206.
(59) de Krom, I.; Bavius, W.; Ziel, R.; McGhee, E. A.; Brown, R. J. C.; Živković, I.; Gačnik, J.; Fajon, V.; Kotnik, J.; Horvat, M.; Ent, H. Comparability of calibration strategies for measuring mercury concentrations in gas emission sources and the atmosphere. *Atmos. Meas. Tech.* **2021**, *14* (3), 2317−2326.
(60) Dumarey, R.; Brown, R. J.; Corns, W. T.; Brown, A. S.; Stockwell, P. B. Elemental mercury vapour in air: the origins and validation of the 'Dumarey equation'describing the mass concentration at saturation. *Accreditation and quality assurance* **2010**, *15* (7), 409−414.
(61) Huber, M. L.; Laesecke, A.; Friend, D. G. Correlation for the vapor pressure of mercury. *Ind. Eng. Chem. Res.* **2006**, *45* (21), 7351−7361. Article. Scopus.
(62) Lyman, S. N.; Gustin, M. S.; Prestbo, E. M.; Kilner, P. I.; Edgerton, E.; Hartsell, B. Testing and Application of Surrogate Surfaces for Understanding Potential Gaseous Oxidized Mercury Dry Deposition. *Environ. Sci. Technol.* **2009**, *43* (16), 6235−6241.
(63) Gratz, L.; Ambrose, J.; Jaffe, D.; Knote, C.; Jaeglé, L.; Selin, N.; Campos, T.; Flocke, F.; Reeves, M.; Stechman, D.; Stell, M.; Weinheimer, A.; Knapp, D. J.; Montzka, D. D.; Tyndall, G.; Mauldin, R. L.; Cantrell, C. A.; Apel, E. C.; Hornbrook, R. S.; Blake, N. Airborne observations of mercury emissions from the Chicago/Gary urban/industrial area during the 2013 NOMADSS campaign. *Atmos. Environ.* **2016**, *145*, 415−423.
(64) Gratz, L. E.; Ambrose, J. L.; Jaffe, D. A.; Shah, V.; Jaeglé, L.; Stutz, J.; Festa, J.; Spolaor, M.; Tsai, C.; Selin, N. E.; Song, S.; Zhou, X.; Weinheimer, A. J.; Knapp, D. J.; Montzka, D. D.; Flocke, F. M.;

https://doi.org/10.1021/acs.est.4c02209
Environ. Sci. Technol. XXXX, XXX, XXX−XXX

Campos, T. L.; Apel, E.; Hornbrook, R.; Blake, N. J.; Hall, S.; Tyndall, G. S.; Reeves, M.; Stechman, D.; Stell, M. Oxidation of mercury by bromine in the subtropical Pacific free troposphere. *Geophys. Res. Lett.* **2015**, *42*, 10494−10502.

(65) Ambrose, J. L.; Gratz, L. E.; Jaffe, D. A.; Campos, T.; Flocke, F. M.; Knapp, D. J.; Stechman, D. M.; Stell, M.; Weinheimer, A. J.; Cantrell, C. A.; Mauldin, R. L. Mercury emission ratios from coal-fired power plants in the Southeastern United States during NOMADSS. *Environ. Sci. Technol.* **2015**, *49* (17), 10389−10397.

(66) Coulter, M. A. Minamata convention on mercury. *International Legal Materials* **2016**, *55* (3), 582−616.

(67) Gratz, L.; Lyman, S.; Elgiar, T.; Hallar, A. G. *Measurements of atmospheric mercury, trace gases, aerosols, and meteorology at Storm Peak Laboratory, Colorado, in 2021 and 2022*; Zenodo, 2024. DOI: 10.5281/zenodo.10699270.

https://doi.org/10.1021/acs.est.4c02209
Environ. Sci. Technol. XXXX, XXX, XXX−XXX